A genetic screen in zebrafish identifies the mutants *vps18*, *nf2* and *foie gras* as models of liver disease

Kirsten C. Sadler[1,*], Adam Amsterdam[1], Carol Soroka[2], James Boyer[2] and Nancy Hopkins[1]

[1]Center for Cancer Research, Massachusetts Institute of Technology, Cambridge MA 02139, USA
[2]Department of Internal Medicine and Yale Liver Center, Yale University School of Medicine, New Haven, CT 06520-8019, USA
*Author for correspondence (e-mail: kirsten_sadler_phd98@post.harvard.edu)

Accepted 24 May 2005

Development 132, 3561-3572
Published by The Company of Biologists 2005
doi:10.1242/dev.01918

Summary

Hepatomegaly is a sign of many liver disorders. To identify zebrafish mutants to serve as models for hepatic pathologies, we screened for hepatomegaly at day 5 of embryogenesis in 297 zebrafish lines bearing mutations in genes that are essential for embryonic development. Seven mutants were identified, and three have phenotypes resembling different liver diseases. Mutation of the class C vacuolar protein sorting gene *vps18* results in hepatomegaly associated with large, vesicle-filled hepatocytes, which we attribute to the failure of endosomal-lysosomal trafficking. Additionally, these mutants develop defects in the bile canaliculi and have marked biliary paucity, suggesting that *vps18* also functions to traffic vesicles to the hepatocyte apical membrane and may play a role in the development of the intrahepatic biliary tree. Similar findings have been reported for individuals with arthrogryposis-renal dysfunction-cholestasis (ARC) syndrome, which is due to mutation of another class C vps gene. A second mutant, resulting from disruption of the tumor suppressor gene *nf2*, develops extrahepatic choledochal cysts in the common bile duct, suggesting that this gene regulates division of biliary cells during development and that *nf2* may play a role in the hyperplastic tendencies observed in biliary cells in individuals with choledochal cysts. The third mutant is in the novel gene *foie gras*, which develops large, lipid-filled hepatocytes, resembling those in individuals with fatty liver disease. These mutants illustrate the utility of zebrafish as a model for studying liver development and disease, and provide valuable tools for investigating the molecular pathogenesis of congenital biliary disorders and fatty liver disease.

Key words: Hepatomegaly, Biliary paucity, Choledochal cyst, Steatosis, Hepatogenesis, Zebrafish

Introduction

Chronic liver disease is responsible for over 27,000 deaths/year in the USA (National Center for Health Statistics, 2004). This number is predicted to rise because of the association of liver disease with obesity: as the numbers of obese individuals in the USA approaches one-third of the population, the incidence of fatty liver has been estimated to affect ~25% of US citizens (Neuschwander-Tetri and Caldwell, 2003). Several hepatobiliary diseases are hereditary or result from developmental defects, especially those presenting in children, such as metabolic disorders and bile stasis (cholestasis) resulting from paucity of bile ducts (Kelly and McKiernan, 1998; Pall and Jonas, 2005). However, with the exception of a few well-known cases, there is a wide chasm between the clinical and molecular understanding of these diseases.

The power of zebrafish to study vertebrate development is well appreciated, and many disease models have emerged from studies with this organism (Rubinstein, 2003). There are several advantages to using zebrafish embryos to develop models of liver diseases. First, in addition to the embryological and genetic benefits of zebrafish, the liver is not the site of embryonic hematopoiesis as it is in mammals, and therefore mutants in liver size or structure will not have the confounding phenotype of hematopoietic dysfunction. Second, the zebrafish embryo survives on yolk for the first 3-4 days of development, after which its digestive system is fully functional and the embryonic fish begins feeding on day 5. Thus, not only is embryogenesis rapid, but the development of a physiologically functional liver occurs within the span of a few days. This provides the opportunity to carry out an embryonic screen to identify mutants that are defective in either liver development or function, or both. Third, baring minor differences, the anatomy, function, organization and cellular composition of adult zebrafish and mammalian livers are virtually the same (Hinton and Couch, 1998; Rocha et al., 1994; Wallace and Pack, 2003), as is the histopathology of fatty liver (steatosis), cholestasis and neoplasia (Amatruda et al., 2002; Spitsbergen et al., 2000) (J. Glickman, personal communication), allowing direct comparison between zebrafish and mammalian liver disease processes. Indeed, recent work has demonstrated that genes that underlie Alagille Syndrome, a pediatric disorder that results in a paucity of intrahepatic bile ducts, among other defects, play an important role in zebrafish biliary development (Lorent et al., 2004). Finally, although the early stages of hepatogenesis are relatively well understood and are similar in mice and zebrafish (Duncan, 2003; Field et al., 2003; Ober et al., 2003), less is known in either system about the final stage of hepatogenesis – hepatic outgrowth. Therefore, the zebrafish

is an excellent system in which to screen for embryonic mutants with large livers (hepatomegaly), for it holds the potential of uncovering both developmental and pathological processes that contribute to this phenotype.

Our laboratory has used insertional mutagenesis to generate over 400 lines of zebrafish bearing mutations in 315 genes that are essential for embryonic development, and the mutated gene has been cloned for each line (Amsterdam et al., 2004; Golling et al., 2002). We calculate that this represents ~22% of the total number of zygotic genes that are essential, as determined genetically, between days 1 and 5 of development (Amsterdam et al., 2004).

We developed a tool to screen day 5 embryos for abnormalities in liver size. Seven mutants with hepatomegaly were identified out of the 297 lines screened. Although several of the mutants may be defective in the regulation of hepatic outgrowth, three of them [*vps18*, *neurofibromatosis 2* (*nf2*) and *foie gras* (*fgr*; *flj12716l* – Zebrafish Information Network)] demonstrate signs of hepatic pathology. Mutation in the *vps18* gene (which is required for endosomal trafficking to acidic organelles) results in albinism and hepatomegaly associated with enlarged hepatocytes, malformation of the bile canaliculi (which is the site of bile secretion at the hepatocyte apical membrane) and biliary paucity. Whereas the pigmentation defect and hepatocyte enlargement can be attributed to the failure to traffic endosomes to the correct intracellular compartment, the canalicular defect probably reflects a defect in the formation of the hepatocyte apical membrane. The hepatobiliary phenotypes seen in this mutant resemble the hepatic signs of individuals with arthrogryposis-renal dysfunction-cholestasis (ARC) syndrome, which is caused by mutation of *vps33B* (Gissen et al., 2004), a gene that interacts with *vps18* (Kim et al., 2001; Peterson and Emr, 2001; Sriram et al., 2003). Second, mutation of *nf2* results in hepatomegaly associated with choledochal cyst formation, and we hypothesize that this results from deregulated biliary cell proliferation. Third, *fgr* mutants develop severe steatosis and we propose this mutant as the first non-mammalian model of a fatty liver disease.

Materials and methods

Animal husbandry and embryo collection

The collection of mutants used in this study were generated, maintained and bred as described (Amsterdam and Hopkins, 1999; Amsterdam et al., 2004). At least five wild-type and five mutant embryos from clutches containing healthy embryos were fixed in formalin overnight at 4°C, washed with PBST (PBS + 0.1% Tween 20) and dehydrated in methanol.

CY3-SA labeling

The labeling protocol was modified from that developed by C. Semino (Phylonix Pharmaceuticals). Embryos were rehydrated through a graded series of methanol to PBST, bleached with 10% H_2O_2/0.5× SSC/0.5% formamide for 12 minutes and blocked with PBST/10% BSA for 1 hour at room temperature. Embryos were incubated with CY3-SA (Sigma; 1:500) in a dark chamber for 2 hours at room temperature, washed with PBST and stored in 80% glycerol.

Embryos were viewed on a Leica MZFLIII stereomicroscope equipped with a fluorescent attachment and scored for liver size, shape, number of lobes as well as for labeling and morphology of the gut. Mutants with hepatomegaly had a left lobe that was visually estimated as greater than ~20% larger than that of their phenotypically wild-type siblings. In each case, the general morphological phenotype has been shown to be tightly linked to a single viral insertion (Golling et al., 2002), and the liver phenotype was always associated with the general morphological phenotype. The mutants were coded, scored blind and only decoded after the phenotype had been observed in at least four clutches. Images were obtained on a Zeiss Axioplan 2 using OpenLab software (Improvision, Lexington, MA).

Morpholino injection

Approximately 0.5-2.0 nl of the following morpholinos at the indicated concentrations were injected into one-cell embryos: *vps18* (1 mM) ATTGATCCAGAATAGATGCCATTGC; *nf2* (0.5 mM) TCAGACCCAAATTGACATAGTGAC; *fgr* (0.05 mM) GAGATCCCATTGCGCTGGACTCATG.

RT-PCR

Day 5 wild-type and mutant embryos from each line were collected and RNA was extracted using the RNAEasy kit (Qiagen). Oligo dT primed cDNA from the RNA equivalent of two embryos was created using the SuperScript II RT Kit (Invitrogen). PCR reactions (30 μl) contained 0.25% of the cDNA reaction, 1× buffer, 0.4 mM $MgCl_2$, 0.2 μM dNTPs, 0.5 μl Taq polymerase (Invitrogen) and 0.4 μM of each primer, and the reaction was carried out for 30 cycles. PCR products were run on a 1.2% agarose gel containing 1 μg/ml ethidium bromide. Primers sequences, 3′ to 5′: fgr-F CTTGCCCCATGAGGTATGAGCAC, fgr-R TGTTGAGCTGAGGGAGGACT; vps18-F CTGGAGGTTGAACGTGGTTT, vps18-R GCAGGAGCAAGAAGTGGAAC; nf2-F CAACCCCACAACAAGCTGAGC, nf2-R GAAGATCGGCTGTTTCCTCAGAG; Actin-F CATCAGCATGGCTTCTGCTCT, Actin R- GCAGTGTACAGAGACACCC.

Histology and electron microscopy

Embryos were fixed in 4% paraformaldehyde for 4 hours at room temperature, washed and dehydrated as described above and embedded in histogel (Richard-Allen Scientific) and then in paraffin. Serial sections (4 μm) were cut and stained with Hematoxylin and Eosin, photographed on a Leica DMRB microscope mounted with a QImaging Retiga EXi digital camera and processed using Adobe Photoshop 5.0.

Embryos for electron microscopy were fixed over night in Karnovsky's fixative (0.1 M cacodylate/2.5% gluteraldehyde/2% formaldehyde/0.85 M $CaCl_2$ pH 7.4) and processed by the Renal Pathology Service at the Brigham and Woman's Hospital (Boston, MA).

Tissue immunolocalization

Day 5 and 7 embryos were anesthetized and embedded in OCT Compound (Tissue Tek, Sakura Fintek), frozen on dry ice and 10 μm sections were cut. Sections were thawed and fixed for 10 minutes with acetone cooled to –20°C. Non-specific sites were blocked with 1% BSA in PBS containing 0.05% Triton X100 and was incubated with 2 hours at room temperature with a 1:100 dilution of monoclonal antibody to P-glycoprotein (Mdr1 and 3, clone C219; Signet laboratories, Dedham, MA). Sections were washed and incubated with Cy3-SA (1:250; Sigma) and Alexa 488 anti-mouse IgG (1:1000; Molecular probes, Eugene, OR) for 1 hour at room temperature. Images were acquired on a Zeiss LSM 510 confocal microscope and processed using Adobe Photoshop.

PED-6 labeling

Day 7 embryos were bathed in 0.3 μg/ml PED6 (Molecular Probes) for 2 hours at 28°C and imaged on a Ziess Axioplan 2. Over 30 mutant, wild-type and morphant embryos were scored for incorporation of the dye into the gallbladder and for the size of the common bile duct.

Histological measurements

Lysosomes and nuclei were counted in 5 thin (1 μm), Toluidine Blue stained Epon sections through the liver of day 5 *vps18* mutant embryos and their phenotypically wild-type siblings.

For each line with hepatomegaly, the hepatocyte internuclear distance was determined from Hematoxylin and Eosin sections. Ten images at 1000× magnification from at least two wild-type and three mutant embryos from the same clutch were collected and the distance between adjacent cell nuclei was measured for 125-175 hepatocytes using Openlab. T-tests were performed on each wild-type-mutant pair; *P*-values <0.001 were considered to be significant.

Results

The hepatomegaly screen

Our laboratory has used viral insertional mutagenesis to generate a collection of over 400 zebrafish lines that are mutated in 315 recessive embryonic lethal genes. The gene bearing the mutagenic insert has been cloned for each line and we estimate that we have achieved ~22% saturation (Amsterdam et al., 1999). As many human genetic diseases are attributed to mutation of one allele of an essential gene that, when homozygously deleted, results in embryonic or neonatal mortality, we envisioned our collection as a pool of potential models for human genetic diseases. Indeed, a recent screen of our collection for mutants that develop kidney cysts has revealed a number of genes that may be important in this disease in humans (Sun et al., 2004).

Hepatomegaly is one of the most common and obvious signs of liver disease. Therefore, hepatomegaly in day 5 zebrafish embryos could be a sign of liver pathology. Alternatively, hepatomegaly could develop from a deregulated liver growth during hepatic outgrowth, and such mutants would be valuable for understanding this final phase of liver development.

We developed a technique to specifically label the liver so as to carry out a large scale screen using fixed material. As biotin serves as a cofactor for a number of liver enzymes (Moss and Lane, 1971), it is found at high levels in hepatocytes. We found that streptavidin conjugated to the fluorophore CY3 (CY3-SA) labels the liver in day 5 embryos (Fig. 1A,B). Additionally, CY3-SA labels the intestinal epithelia and yolk because of a high concentration of biotin in these tissues (Fig. 1A,B).

We used CY3-SA to screen nearly all of the lines of our collection to identify those which develop hepatomegaly on day 5 of development. Out of the 297 lines that were available to be screened, seven mutants with hepatomegaly were identified (Fig. 1B; Table 1), representing 2.4% of all mutants screened. Given that our collection represents ~22% of all embryonic essential genes, and that this screen covered 94% of our collection (i.e. ~21% of all embryonic essential genes), we estimate that a total of ~33 of the essential genes could result in this phenotype. The genes underlying hepatomegaly each appear to function in different cellular processes, although two (*fgr* and *pté*) have no defined cellular or biochemical function (i.e. 'novel'; Table 1).

Hepatomegaly in each mutant was confirmed by in situ hybridization with the liver-specific marker, fatty acid binding protein 1 (K.C.S., unpublished) (Her et al., 2003). Morphological and histological analysis did not reveal organomegaly in any other tissue (K.C.S., unpublished). The yolk is consumed by day 5 in most wild-type embryos;

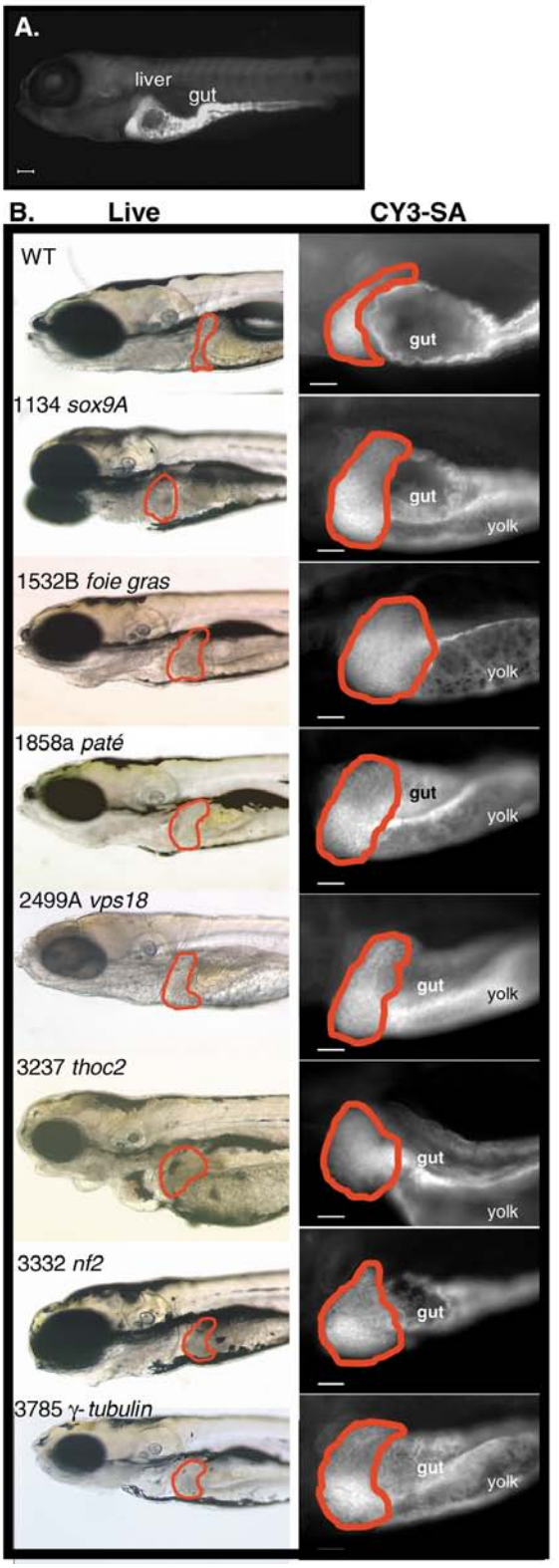

Fig. 1. Seven mutants develop hepatomegaly by day 5 of development. (A) CY3-SA specifically labels the liver and gut in day 5 wild-type embryos. Scale bar: 100 μm. (B) Live images (left) and CY3-SA-labeled livers of wild-type and mutant embryos. The liver is outlined in red. The gut is indicated in each embryo, except *fgr*, which has an underdeveloped gut that does not label with CY3-SA. Scale bars: 50 μm.

Table 1. Zebrafish mutants with embryonic hepatomegaly

Line	Gene	Mutant name	Gene ontogeny and function	Cell size	Extracellular space	Pathology
hi^{2499A}	*vps18*	*vps18*	Conserved to yeast; vacuolar sorting protein	Large	Expanded	ARC syndrome-like
hi^{3332}	*nf2*	*nf2*	Conserved in metazoa; tumor suppressor	Wild type	Expanded	Choledochal cysts type I and II
hi^{1532B}	*foie gras*	*foie gras* (*fgr*)	Conserved in metazoa; novel	Large	Wild type	Steatosis
hi^{3237}	*thoc2*	*thoc2*	Conserved to yeast; couples mitotic recombination, transcription and RNA export	Large	Wild type	None observed
hi^{3785}	*γ-tubulin*	*γ-tub*	Conserved to yeast; centrosome protein	Large	Wild type	None observed
hi^{1134}	*sox9a*	*jelly fish* (*jef*)	Conserved in metazoa; tissue specific transcription factor	Wild type	Wild type	None observed
hi^{1858A}	*paté*	*paté* (*pté*)	Conserved to yeast; novel	Wild type	Wild type	None observed

The cellular phenotype and deduced hepatic pathology is indicated.

however, we observe that most of the mutant embryos in our collection, including the embryos identified by this screen, do not fully use the yolk (Fig. 1B). CY3-SA also labels the intestinal epithelia and we used this to score gut morphology for each mutant. The gut develops normally in *sox9a*, *vps18* and *nf2*, is slightly underdeveloped in *pté*, *thoc2* and *γ-tub*, and is severely abnormal in *fgr*.

Diagnosis of liver disease relies upon clinical presentation, biochemical measurement of liver function and assessment of the pathology from a liver biopsy. We used histological analysis to identify signs of pathology in each mutant, and to assess the hepatic architecture, cell composition and cell size. The cellular phenotype of each mutant is described in Table 1. Four mutants (*vps18*, *fgr*, *γ-tub* and *thoc2*) were identified as having enlarged hepatocytes, which was confirmed by a quantitative measure of cell size (Fig. 2). Two mutants (*vps18* and *nf2*) contained large spaces in the extracellular hepatic matrix (Fig. 2A; see Fig. 5). Further analysis suggested that this is associated with biliary defects in both cases (see below). In two mutants (*sox9a* and *pté*), the hepatocytes are the same size as wild type (Fig. 2B) and there is no evidence of expansion of the extracellular space; in these cases, hepatomegaly may develop due to unregulated proliferation of hepatocytes. Signs of hepatobiliary pathology were detected in three mutants (*vps18*, *nf2* and *fgr*), and we further characterized each of these.

vps18 is required for pigmentation, endosomal transport in hepatocytes, formation of the bile canaliculi and intrahepatic biliary development: a model for the hepatic signs of ARC syndrome

Mutants from *hi*^{2499A} contain an insertion in the *vps18* gene following nucleotide 2236 (Fig. 3A). This insertion results in an abrogation of the *vps18* message in mutant embryos (Fig. 3B). *vps18* message is present in oocytes (i.e. immature and unfertilized eggs) and in embryos on days 1-5 of development (K.C.S., unpublished), and only the zygotically transcribed message is affected in the hi^{2499A} mutants. Injecting high concentrations of a morpholino directed against the start site of the *vps18* gene to knock-down the translation of the maternal message results in pigmentation defects (Fig. 3A) and, in some embryos, causes global developmental defects early in development (K.C.S., unpublished). Lower concentrations of the morpholino do not interfere significantly with pigmentation or development, but do cause hepatomegaly (Fig. 4A). These data indicate that the pigmentation defects and hepatomegaly observed in mutants from hi^{2499A} can be attributed to the loss of *vps18* function. Thus, we hereafter refer to the *hi*^{2499A} mutants as *vps18*.

vps18 is a class C vacuolar protein sorting gene (Raymond

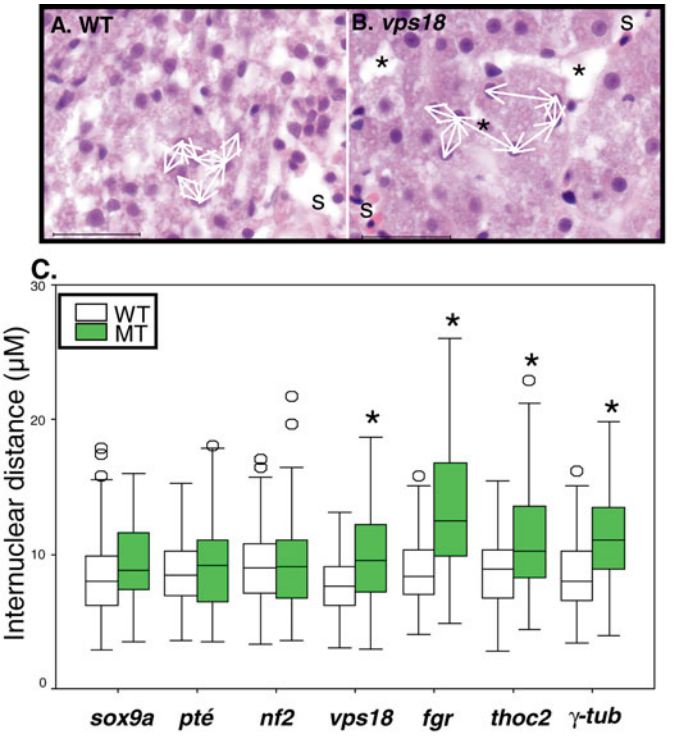

Fig. 2. Four mutants with hepatomegaly have increased internuclear distance. (A,B) The internuclear distance between adjacent hepatocytes (white arrows) illustrated in wild-type (A) and *vps18* (B) hepatocytes. Cells separated by sinusoids (s) or large extracellular gaps (*) were excluded. Scale bar: 50 μm. (C) The hepatocyte internuclear distance was measured for wild-type and mutant embryos from each line and plotted in box and whisker plots. The 25th, 50th (median) and 75th percentiles are indicated as the horizontal lines of the box, with the 10th and 90th percentiles shown as cross bars on lines extending from the boxes. Measurements falling outside of the 10th and 90th percent were considered outliers and are shown as open circles. *P<0.001, as determined by Student's t-test..

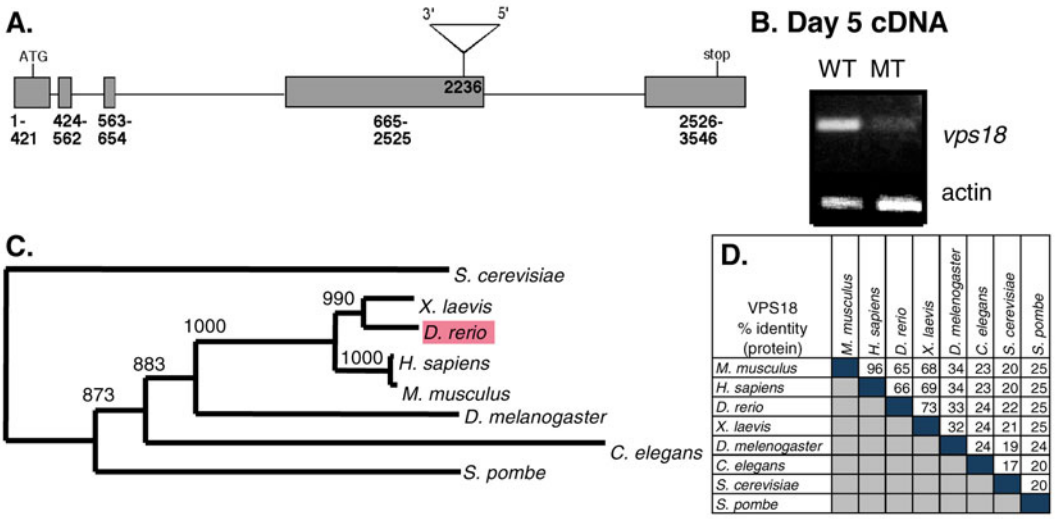

Fig. 3. *hi*^{2499A} mutants contain a mutagenic insertion in the *vps18* gene. (A) Viral insertion in the *vps18* gene at nucleotide 2236. Grey boxes indicate exons, horizontal lines indicate introns. Triangle represents virus. (B) cDNA prepared from day 5 phenotypically wild-type embryos and their mutant siblings from *hi*^{2499A} was amplified with *vps18* and actin primers. (C) Unrooted phylogenetic tree for *vps18*. Bootstrap numbers are indicated. (D) Percent identity matrix for the Vps18 protein.

et al., 1992). The products of the class C genes (*vps11*, *vps16*, *vps18* and *vps33*) direct the targeting, docking and SNARE-mediated fusion of vesicles to the yeast vacuole and animal lysosome (Kim et al., 2001; Peterson and Emr, 2001; Poupon et al., 2003; Raymond et al., 1992; Sato et al., 2000; Srivastava et al., 2000). We carried out a detailed analysis to determine whether this function of the *vps18* gene could account for the two prominent phenotypes displayed by *vps18* mutants: albinism and hepatomegaly.

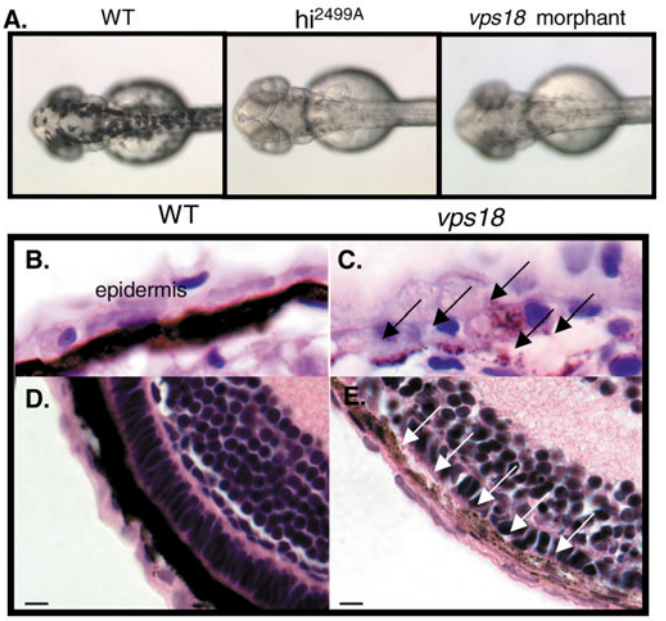

Fig. 4. *vps18* is required for pigment formation. (A) Day 2 *hi*^{2499A} mutants and *vps18* are not pigmented. (B-E) The day 5 epithelium of the skin (B,C) and the retina (D,E) is darkly pigmented in wild-type embryos (B,D), whereas *vps18* mutants (C,E) have sparse pigment granules (arrows). Scale bar: 5 μm.

vps18 is well conserved and has an orthologs in every eukaryotic species examined (Fig. 3C). There is 66% identity between the human and zebrafish, and 33% between zebrafish and *Drosophila* proteins (Fig. 3D), suggesting that the function of *vps18* is conserved between species. Abnormalities in eye pigmentation in the *Drosophila vps18* mutant, *deep orange* (*dor*) (Puckett and Petty, 1980; Sevrioukov et al., 1999) are due to a defect in endosomal trafficking and fusion with the pigment granule (Sevrioukov et al., 1999; Sriram et al., 2003). Although dense pigment granules are seen in the pigmented epithelia of the epidermis and retina of wild-type zebrafish embryos (Fig. 4B,D), *vps18* mutant embryos have only a few irregularly distributed pigment granules in these tissues (Fig. 4C-E). This phenotype resembles the pigmentation defect observed in *dor* mutants, suggesting that the function of *vps18* in pigment granule maturation, which is analogous to lysosome biogenesis, is conserved in these two distantly related animals.

Given that loss of *vps18* function disrupts the trafficking of late endosomes in yeast and mammals (Huizing et al., 2001; Poupon et al., 2003; Srivastava et al., 2000) we examined *vps18* mutant livers to determine whether this same function could account for hepatomegaly that is observed in *vps18* mutants and morphants (Fig. 5A).

Livers in day 5 wild-type embryos consist primarily of hepatocytes, which have a lacey, eosinophilic cytoplasm (Fig. 2A; Fig. 5B). Although sinusoids can be easily identified, bile ducts are never observed in embryonic livers using standard histological methods. Hepatocytes in *vps18* mutant embryos are enlarged (Fig. 2) and contain large cytoplasmic structures resembling vesicles or vacuoles (Fig. 5D). There is less eosinophic material in the *vps18* mutant hepatocytes compared with wild type, and this may reflect the decreased levels of stored glycogen in the *vps18* mutant hepatocytes (K.C.S., unpublished).

We used transmission electron microscopy (TEM) to determine the nature of the cytoplasmic structures seen in *vps18* mutant hepatocytes (Fig. 5E,F). Hepatocytes from wild-

type day 5 embryos contain copious glycogen, which causes the cytoplasm to have a homogeneous, grainy appearance. By contrast, little glycogen is seen in the *vps18* mutant hepatocytes. Instead, large, membrane-bound structures containing proteinacious material and debris were observed (Fig. 5F). These are similar to the aberrant structures seen in yeast and *Drosophila* cells that lack *vps18* (Sevrioukov et al., 1999; Sriram et al., 2003; Srivastava et al., 2000). A failure to deliver endosomal cargo to the lysosome prevents lysosome biogenesis; we found that *vps18* mutant hepatocytes have one-quarter the number of lysosomes of wild type (Fig. 4G). Taken together, these data suggest that *vps18* acts in zebrafish to target endosomes to the pigment granule in melanocytes and to the lysosome in hepatocytes. We conclude that the failure of endosomal-lysosomal targeting causes transport intermediates to build up in the hepatocytes, resulting in hepatocyte enlargement and hepatomegaly.

ARC syndrome is an autosomal recessive disease that affects the liver, kidneys, platelets and neurogenic muscular function (Eastham et al., 2001). Typical hepatic defects include hepatomegaly, intrahepatic biliary paucity and cholestasis associated with mislocalization of canalicular markers (Gissen et al., 2004; Horslen et al., 1994). Recently, Gissen et al. have shown that this disease is due to mutation in another class C vps gene, *vps33B* (Gissen et al., 2004). Given that Vps18 and Vps33B function in the same complex (Huizing et al., 2001; Kim et al., 2001; Peterson and Emr, 2001; Poupon et al., 2003; Raymond et al., 1992; Subramanian et al., 2004), we asked whether biliary defects similar to ARC syndrome occur in *vps18* zebrafish mutants.

vps18 mutant livers contain large spaces in between hepatocytes (Fig. 2A). The spaces are devoid of nucleated red blood cells and were not lined by endothelial cells. We concluded that they were not part of the hepatic microvasculature (sinusoids). In order to determine whether these spaces reflected a defect in the intrahepatic biliary system, we undertook a detailed histological, immunological and ultrastructural examination of the embryonic biliary tree.

Bile is secreted at the hepatocyte apical membrane in a specialized structure called the bile canaliculi (Ujhazy et al., 2001). Bile transporters, such as MDR1, are specifically localized to the canaliculi in mammals (Trauner et al., 1997; Trauner and Boyer, 2003) and in fish (Hemmer et al., 1995; Lorent et al., 2004). In day 5 wild-type zebrafish embryos, MDR1 is localized exclusively to the tube-shaped canaliculi (Fig. 6B,C). By contrast, MDR1 localization in *vps18* mutant livers is punctate (Fig. 6E,F) and the canaliculi are large and round (Fig. 6F, arrows). Importantly, we found MDR1 labeling in the cytoplasm of some *vps18* hepatocytes (box in Fig. 6F), suggesting that it is not trafficked properly to the apical canalicular domain.

In mammals, bile flows from bile canaliculi to bile ducts through the canal of Hering. Teleosts do not appear to have a canal of Hering, but instead the canaliculi empty directly into the lumen of pre-ductules, which are formed by biliary pre-ductal epithelial cells (PDEC), a specialized cell of the intrahepatic biliary tree in teleosts (Hinton and Pool, 1976; Rocha et al., 1994). PDECs form the lumen of the pre-ductule by wrapping around themselves, analogous to capillary formation by endothelial cells (Hinton and Couch, 1998; Hinton and Pool, 1976; Rocha et al., 1994). Although PDECs are reported to express cytokeratin 19 (Lorent et al., 2004; Matthews et al., 2004), a classic marker of biliary epithelial cells, they are not columnar, they lack a basal lamina (Rocha et al., 1994) and they appear less differentiated than the cholangiocytes that form the

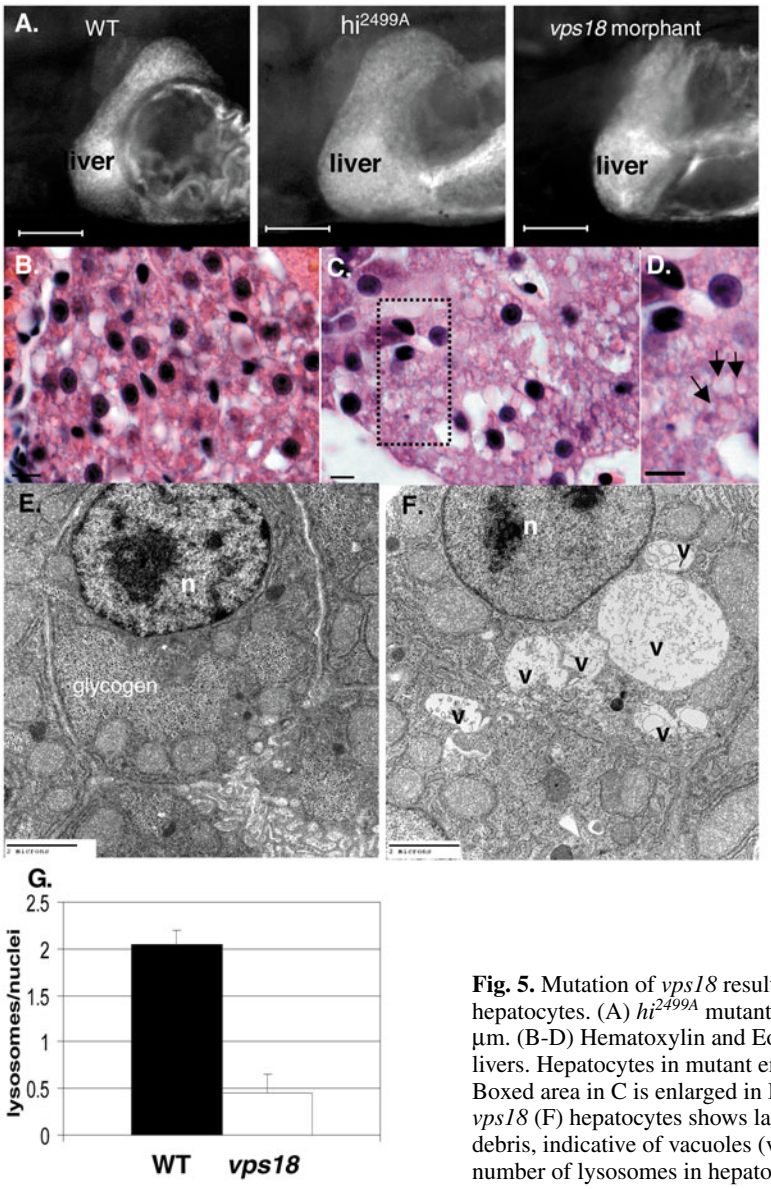

Fig. 5. Mutation of *vps18* results in vesicle accumulation and lysosome depletion in hepatocytes. (A) *hi*^{2499A} mutants and *vps18* morphants develop hepatomegaly. Scale bar: 100 μm. (B-D) Hematoxylin and Eosin staining of day 5 wild-type (B) and *vps18* mutant (C,D) livers. Hepatocytes in mutant embryos are large and accumulate vacuoles (arrows in D). Boxed area in C is enlarged in D. Scale bar: 5 μm. (E,F) TEM of day 5 wild-type (E) and *vps18* (F) hepatocytes shows large, membrane-bound structures proteinacious material and debris, indicative of vacuoles (v) in the mutants. *n*, nucleus. (G) *vps18* mutation reduces the number of lysosomes in hepatocytes. Error bars indicate standard error of the mean.

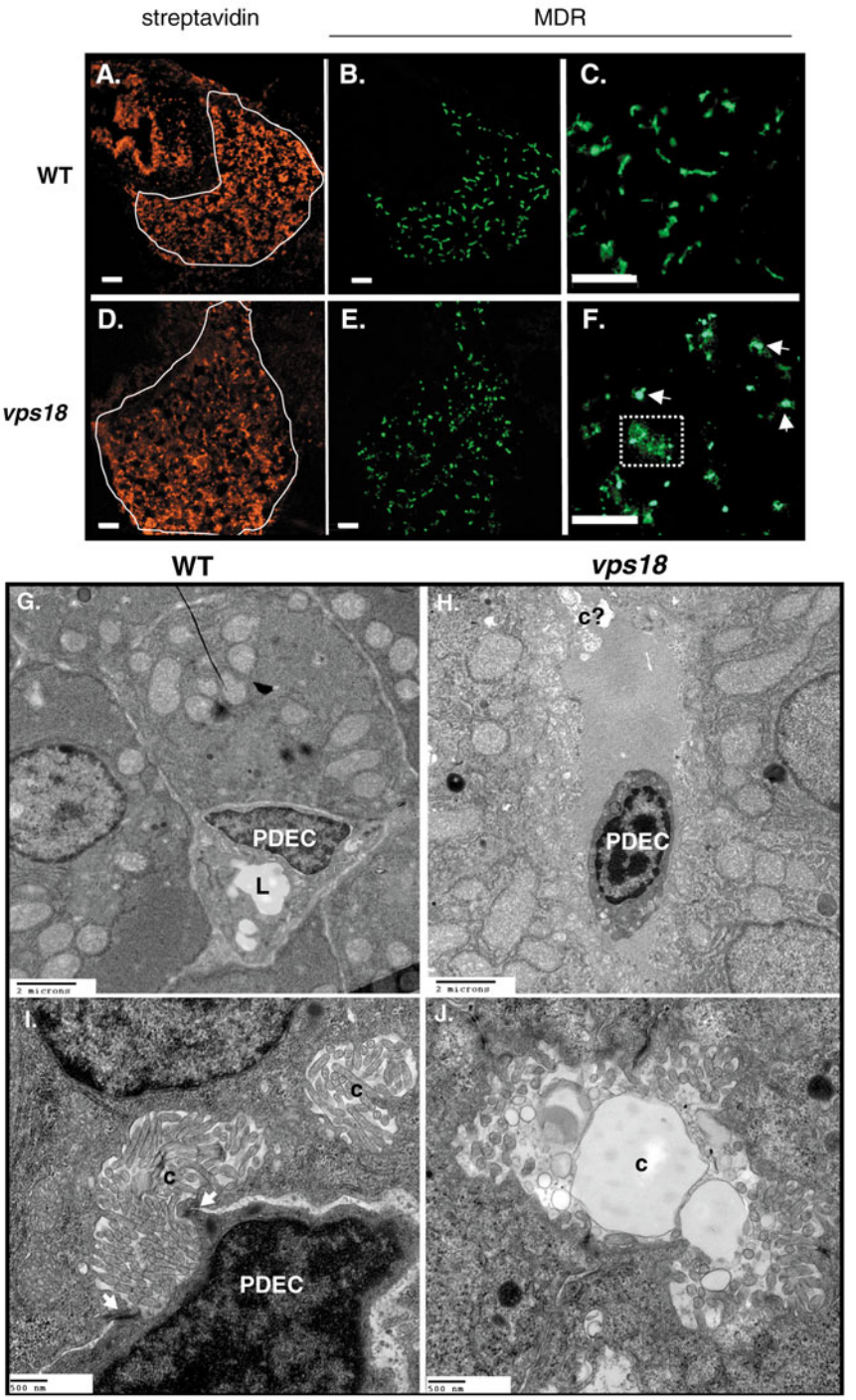

Fig. 6. Mutation in *vps18* results in biliary defects. (A-F) Confocal images of livers from wild-type (top) and *vps18* mutant (bottom) embryos from day 5 (A,B,D,E) and day 7 (C,F) labeled with CY3-SA (A,D) and anti-MDR (B,C,E,F). Some hepatocytes in the mutant embryos retain some MDR in the cytoplasm (box in F). Scale bars: 10 μm. (G-I) TEM of day 5 embryos identifies PDECs as cells adjacent to hepatocytes that collect bile from the canaliculi of neighboring hepatocytes and transport it through their lumen (arrows in I). (H,J) *vps18* mutant livers contain virtually no PDECs, and those that are found do not establish contacts with hepatocytes, are shrunken and have condensed DNA (H). PDEC, pre-ductal epithelial cell; c, canaliculi; c?, putative aberrant canaliculi; L, lumen. Scale bars: 20 μm G,H; 500 nm in I,J.

hepatic duct, gallbladder and common bile duct (Fig. 7G).

We could not identify PDECs by histological or immunological methods, but could readily identify them by TEM as small cells that contain a prominent, multi-lobed nucleus, and are sandwiched between hepatocytes (Fig. 6G). The bile canaliculi in day 5 zebrafish embryos are formed at the apical membrane of 1-4 hepatocytes and are flanked by tight junctions between adjacent hepatocytes (K.C.S., unpublished) and between hepatocytes and PDECs (Fig. 6I). We found that the entire intrahepatic biliary tree in day 5 zebrafish embryos comprises preductules that coalesce at the hepatic duct.

TEM was used to determine whether *vps18* mutants have a defect in PDECs and the bile canaliculi. The number of PDECs in day 5 *vps18* mutant livers is drastically reduced, and those we could identify were shrunken, did not maintain tight junctions with the surrounding hepatocytes and their nuclei contained condensed DNA (Fig. 6H), suggestive of apoptosis. The space seen to surround PDECs in *vps18* mutants may represent the large extracellular spaces observed on histological sections. As in ARC syndrome patients (P. Gissen, personal communication) the extrahepatic biliary tree is not affected in *vps18* mutants (K.C.S., unpublished).

Consistent with the abnormal MDR1 labeling seen in *vps18* mutant livers, there are dramatic defects in the bile canaliculi. Canaliculi in wild-type zebrafish embryos are packed with regularly spaced and evenly shaped microvilli (Fig. 6I), and ultrastructurally appear very similar to canaliculi in mammals. Canaliculi in *vps18* mutants have sparse, blunted microvilli and are distended and contain debris (Fig. 6C,D). This morphology is typically seen in individuals with cholestasis and is identical to those seen in sea lamprey which develop cholestasis during metamorphosis (Sidon and Youson, 1983), suggesting cholestasis may also develop in *vps18* mutants.

Our analysis of *vps18* mutants indicates that the pigmentation defects and hepatomegaly can be attributed to the well characterized function for this gene in endosomal-lysosomal trafficking. In addition, this study has identified a new role for *vps18* in trafficking to the hepatocyte apical plasma membrane and formation of the bile canaliculi. Canalicular malformation (Gissen et al., 2004) and biliary paucity (P. Gissen, personal communication) is an abnormality shared between *vps18* mutants in zebrafish and mutation of the *vps33B* gene in individuals with ARC syndrome. Taken together, these data are consistent with the hypothesis that class C VPS genes are required in trafficking to the bile canaliculi at the hepatocyte apical plasma membrane.

nf2 mutants as a model for choledochal cysts

Choledochal cyst formation is a congenital disorder that is most often detected in childhood, although an increased incidence in adults has recently been reported (Soreide et al., 2004). Cyst classification is based on the site of the cyst and whether both intrahepatic and extrahepatic involvement is detected (Soreide et al., 2004). The etiology of cyst formation is not known. Although most cases are the result of developmental defects, a genetic component is suggested by the occurrence of some familial cases (Behrns et al., 1998; Iwama, 1998; Iwama et al., 1985; Iwata et al., 1998). Choledochal cysts carry a greatly elevated risk for developing cholangiocarcinoma, and although cyst excision diminishes this risk, it is not eliminated (Soreide et al., 2004). This suggests that that cholangiocytes in individuals with choledochal cysts may be predisposed to hyperproliferation and malignant transformation.

The *Nf2* gene in mammals is a tumor suppressor (Lekanne Deprez et al., 1994; McClatchey et al., 1998; Ruttledge et al., 1994; Sanson et al., 1993). Mutants from *hi*^{3332} contain a single viral insertion within the intron preceding the first coding exon of the *nf2* gene (Fig. 7A). This insertion causes a complete abrogation of the *nf2* message in mutant embryos (Fig. 7B). The *nf2* gene has been duplicated in zebrafish to create *nf2a* (subsequently called *nf2*) and *nf2b* genes, which are over 60% identical at the nucleotide level (A.A., unpublished). The *nf2* gene is expressed in oocytes and in embryos through day 5 of development, while the *nf2b* message is detected only in oocytes (K.C.S., unpublished). Injecting embryos with a morpholino that is specific for the *nf2* message phenocopies the biliary phenotype observed in mutants from *hi*^{3332} (see below). Thus, it is unlikely that *nf2b* significantly affects the phenotype of mutants bearing an insertion in the *nf2* gene and we refer to the mutants from *hi*^{3332} as *nf2*.

Mouse embryos homozygously deleted for the *nf2* gene arrest before gastrulation (McClatchey et al., 1997). Our screen indicates that the *nf2* gene is also essential for embryogenesis in zebrafish, although *nf2* mutants have only modest

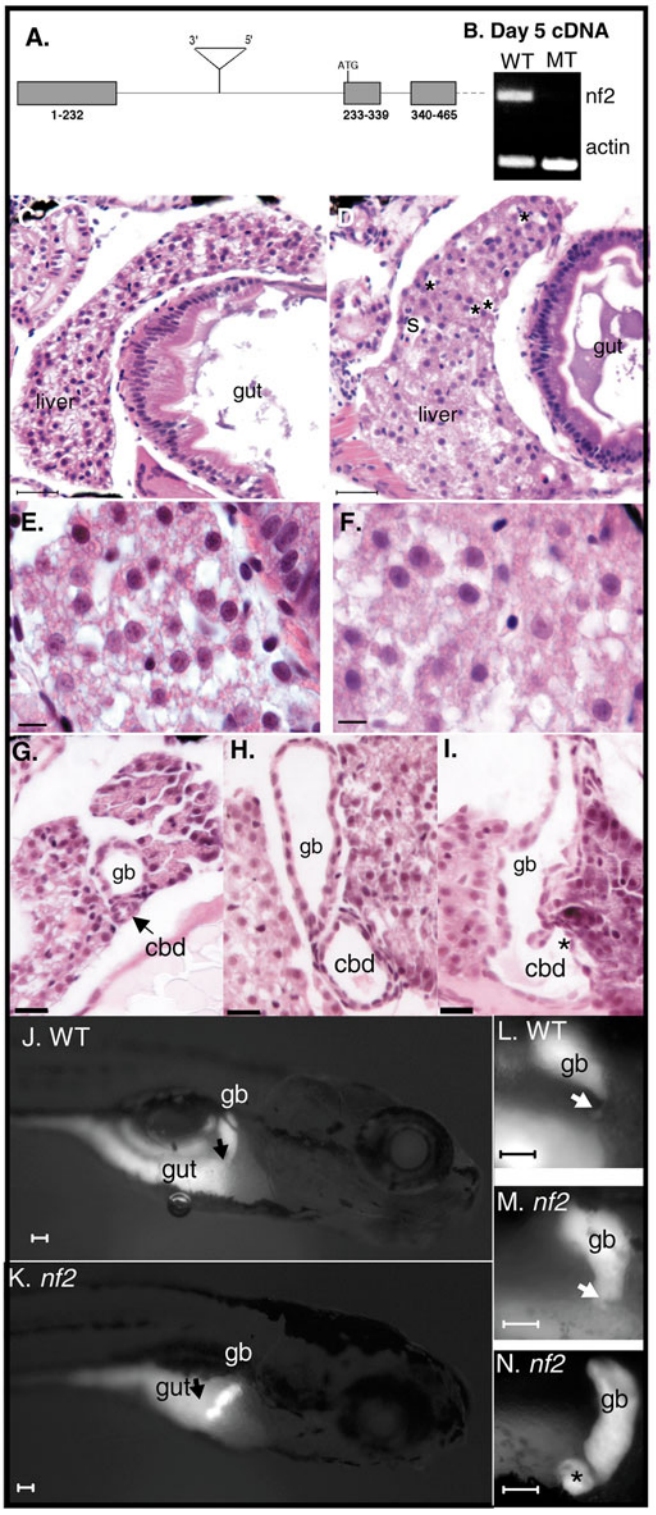

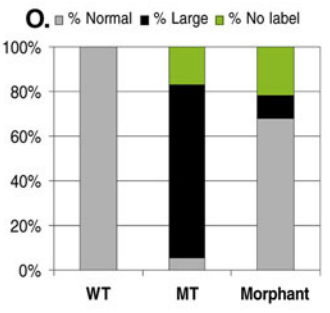

Fig. 7. Mutation of the *nf2* gene results in choledochal cyst formation. (A) *hi*^{3332} mutants contain an insertion in the intron upstream of the start site of the *nf2* gene. Grey boxes indicate exons, lines indicate introns; ATG is the start codon. (B) cDNA prepared from day 5 phenotypically wild-type embryos and their mutant siblings from *hi*^{3332} was amplified *nf2* and actin primers. (C-I) Hematoxylin and Eosin-stained histological sections through wild-type (D,E,G) and mutant (D,F,H,I) liver (C-F), gallbladder and common bile duct (G-I). Other than the large spaces in the mutant livers (asterisk in D), the wild-type and mutant livers appear similar (E,F). The common bile duct is cystic in *nf2* mutant embryos (H,I). The section in I illustrates the gallbladder-ductal junction, and the formation of a diverticuli (asterisk) in the common bile duct of this embryo. Scale bars: 50 μm in C,D; 5 μm in E-I. (J-N) PED6 labeling of wild-type (J,L) and *nf2* mutant (K,M,N) day 7 embryos. The gallbladder is a brightly labeled oblong or spherical organ in wild-type embryos, whereas it is always oblong in mutant embryos. The common bile duct (arrows) is dilated and diverticuli (asterisk in N) form in *nf2* mutant embryos. (O) Quantification of ductal morphology in wild-type, mutant and *nf2* morphant day 7 embryos fed PED6. $P<0.003$ for the comparison of the number of embryos with dilated bile ducts in wild-type and mutant embryos (not shown). Some mutant and morphant embryos do not accumulate any PED6 in their gallbladder (no label). gb, gallbladder; cbd, common bile duct.

morphological defects on day 5 of development, including a small forebrain and hepatomegaly (Fig. 1B). We attribute this difference to the presence of maternal *nf2* message, as injecting a high concentration of a morpholino designed against the *nf2* start site arrests embryos at the one- to two-cell stage.

There is no dramatic hepatocellular phenotype in *nf2* mutant livers, and the size of the hepatocytes are equivalent to wild-type embryos (Fig. 2C, Fig. 7B-E). In some regions of the liver, however, there are large spaces between hepatocytes (Fig. 7D and Table 1). These spaces do not appear to be sinusoids, but may reflect a biliary defect.

The most striking phenotype of *nf2* mutants is the dilated common bile duct (Fig. 7G-N). On histological sections, both the gallbladder and the common bile duct are enlarged compared with wild-type sections through the same plane (Fig. 7G-I), indicating the formation of a type Ic (solitary, cystic) choledochal cyst. In some *nf2* mutant embryos, diverticuli are observed in the cystic ducts (Fig. 7I), indicating the formation of Type II (supraduodenal diverticuli) choledochal cysts. Both of these abnormalities are not accompanied by any obvious morphological or dysplastic change in the cholangiocytes, but there does appear to be an increase in the number of cells forming the duct.

The fluorphor-linked phospholipid, PED6, has been used in zebrafish to visualize the gut and gallbladder in live embryos (Farber et al., 2001). We used PED6 to examine the common hepatic duct in live embryos. All wild-type day 7 embryos incubated in PED6 demonstrate robust fluorescence in the gut and gallbladder, as do the majority of the *nf2* mutants (Fig. 7J,K), although some of the mutants and *nf2* morphants fail to transfer any PED6 to the gallbladder (i.e. 'no label' in Fig. 7O) The common bile duct can barely be detected as a string of fluorescence connecting the gallbladder and the gut in wild-type embryos (Fig. 7M,O), while 80% of the *nf2* mutant embryos have a markedly distended bile duct (Fig. 7N,O). Roughly half of the mutant embryos also form a diverticuli from the common bile duct (Fig. 7N), confirming the histological phenotype (Fig. 7I). Obstruction can result in biliary dilation; however, serial sectioning through the common bile duct *nf2* embryos as well as pulse chase experiments with PED6 did not reveal any obstruction distal to the cyst (K.C.S., unpublished). Taken together, these histological and physiological data indicate that the *nf2* gene in zebrafish is involved in bile ductogenesis, and that loss of *nf2* function results the formation of type I and type II choledochal cysts.

Fgr mutants as a model for steatosis

Steatosis is a common cause of hepatomegaly (Neuschwander-Tetri and Caldwell, 2003). Approximately 10% of individuals with steatosis that have no history of alcohol abuse progress to develop the severe fatty liver disease non-alcoholic steatohepatitis (NASH), characterized by hepatomegaly, deranged liver function and steatosis, resulting in hepatocyte death and inflammation that can develop into cirrhosis (Diehl, 2001). It is not clear why only a subset of individuals progress from simple steatosis to NASH, but genetic predisposition may play an important role. Indeed, while steatosis and NASH are usually associated with obesity, there are well documented cases of familial NASH (Neuschwander-Tetri and Caldwell, 2003; Struben et al., 2000; Willner et al., 2001), indicating a genetic component to this disease.

hi^{1532B} mutants develop massive hepatomegaly, a failure of gut development and abnormalities lower jaw and the fin morphology (Fig. 1). *hi*^{1532B} mutants contain an insertion in the intron between exons 11 and 12 of a novel gene which we named *foie gras* (*fgr*). The virus contains a 172 bp gene-trap cassette and in *hi*^{1532B} mutant embryos, the gene-trap is spliced in frame following bp 1287 of the *fgr*-coding sequence (Fig. 8A). This results in a frame shift that creates a stop codon immediately following the gene trap (Fig. 8A). Thus, mutant embryos from *hi*^{1532B} contain only transcript that encodes the allele with the gene trap (Fig. 8B, mutant band), while phenotypically wild-type siblings from the same clutch, of which two-thirds of these embryos are heterozygotes, have transcript encoding the wild-type allele as well as a small amount of the mutant allele (Fig. 8B). Injection of a morpholino designed against the start codon of the *fgr* message phenocopies the *hi*^{1532B} mutants (K.C.S., unpublished), leading us to conclude that the viral insertion in this gene results in a loss of *fgr* function. Henceforth, we refer to mutants from *hi*^{1532B} as *fgr*.

Histological analysis of *fgr* mutant livers revealed enlarged hepatocytes which are filled with large, clear vesicles (Fig. 8C-D), suggestive of fat accumulation. Cells with fragmented nuclei and cell corpses, indicative of cell death, were frequently seen in *fgr* mutant livers (Fig. 8D), but never in wild type. Using the lipid stain, oil red O, we found a substantial amount of lipid accumulation in *fgr* mutant livers (Fig. 8E,F). Thus, some of the hallmark signs of NASH – hepatocytes enlargement, steatosis and an increase in hepatocyte death – were all observed in *fgr* mutants. The exception is the conspicuous absence of inflammation in *fgr* mutant livers, despite the marked cell death. We attribute this to the incomplete maturation of the zebrafish immune system at this stage of development. Nevertheless, mutation of the *fgr* gene, for which the function has not yet been determined in any organism, results in hepatomegaly associated with a phenotype that resembles NASH, and may serve as a non-mammalian model for studying this widespread and important disease.

Discussion

We have undertaken a forward genetic screen in zebrafish to identify mutants which develop hepatomegaly – a common sign of many liver pathologies – in an effort to develop zebrafish models of liver diseases. This study has not only identified three such models, but also demonstrated important roles for several new genes in liver development, physiology and pathology. We found signs of hepatic pathology in three mutants, and propose *vps18* as a model for the hepatobiliary defects observed in ARC syndrome, *nf2* as a model for choledochal cysts and *fgr* as a model for fatty liver disease.

The role of *vps18* in vesicle trafficking to the vacuole in yeast (Peterson and Emr, 2001; Sato et al., 2000; Srivastava et al., 2000), to the pigment granule and synapse in *Drosophila* (Narayanan et al., 2000; Sevrioukov et al., 1999; Shestopal et al., 1997) and to the lysosome in mammals (Huizing et al., 2001; Kim et al., 2001; Poupon et al., 2003) has been well defined. Although data from *Drosophila* (Counce, 1956) and our morpholino experiments suggest an essential role for *vps18* early in development, we believe the maternal contribution of RNA, protein and nutrients in zebrafish enables the *vps18*

mutants, and others (such as *γ-tub*) that bear mutation in a cell-essential gene, to survive the first few days of development.

We found that the two prominent morphological phenotypes of the *vps18* mutant zebrafish embryo – pigmentation and hepatomegaly – could both be attributed to the well characterized role for the Vps18 protein in trafficking to the pigment granule or lysosome. It is likely that hepatomegaly develops in these embryos due to the accumulation of pre-lysosomal vesicles in the hepatocyte cytoplasm causing cell enlargement. Further analysis of this mutant, however, suggests that this protein also functions in trafficking to the hepatocyte apical membrane and formation of the canaliculi, and is required for development of the intrahepatic biliary tree. Alternatively, biliary paucity in these mutants could develop because of damage and death of the PDECs (i.e. biliary atresia), possibly as a result of cholestasis which may develop in these mutants. Biliary paucity and canalicular defects are also seen in individuals who suffer from ARC syndrome (P. Gissen, personal communication), which is due to homozygous mutation of the *vps33B* gene (Gissen et al., 2004). Given that the Vps18 and Vps33B proteins act as part of the same complex in yeast and in animals (Huizing et al., 2001; Kim et al., 2001; Peterson and Emr, 2001; Sato et al., 2000) in trafficking to the vacuole and lysosome, and that vesicle targeting and fusion with the apical membrane in hepatocytes involves a SNARE-dependent process that requires other VPS genes (Tuma and Hubbard, 2001,), our data support the hypothesis that *vps18* and *vps33B* are also required for trafficking to the apical membrane.

Interestingly, morpholino knock down of *vps33B* message in zebrafish embryos reportedly results in cholestasis and biliary paucity (M. Pack, personal communication). Given that the phenotypes of *vps18* mutants, *vps33B* morphants and individuals with ARC syndrome are not identical [i.e. *vps18* mutants do not have signs of arthrogryposis or renal dysfunction (K.C.S., unpublished)] and *vps33B* zebrafish morphants and individuals with ARC syndrome are normally pigmented (M. Pack and P. Gissen, personal communication), we propose that *vps18* and *vps33B* may take on tissue specific roles or that functional redundancy exists in some tissues but not in others. Our data suggest, however, that the hepatic phenotype of *vps18* mutants and individuals with ARC syndrome are very similar, and that this is due to the interruption of the same molecular complex involved in two trafficking pathways in hepatocytes. We thus propose the *vps18* zebrafish mutant as a model for studying the hepatic signs of ARC syndrome.

The other mutant we identified to have hepatomegaly associated with a biliary defect bears an inactivating mutation in the *nf2* gene. These mutants develop type Ic and type II choledochal cysts. Although there are signs of intrahepatic biliary pathology in *nf2* mutants, unlike *vps18*, the PDECs in *nf2* mutants are not atretic, but on the contrary, may be hyperproliferative (K.C.S., unpublished). Indeed, the fact that intrahepatic bile ducts are often hyperproliferative in individuals with extrahepatic choledochal cysts (Nambirajan et al., 2000) and choledochal cysts carry a predisposition to cholangiocarcinoma (Soreide et al., 2004) indicates a strong link between cyst formation and proliferation control. It is possible that in the absence of *nf2*, there may be unregulated proliferation of a bi-potential cell that can give rise to both hepatocytes and biliary cells, analogous to an oval cell (Newsome et al., 2004). This could account for both the increase in biliary cells and hepatomegaly observed in *nf2*

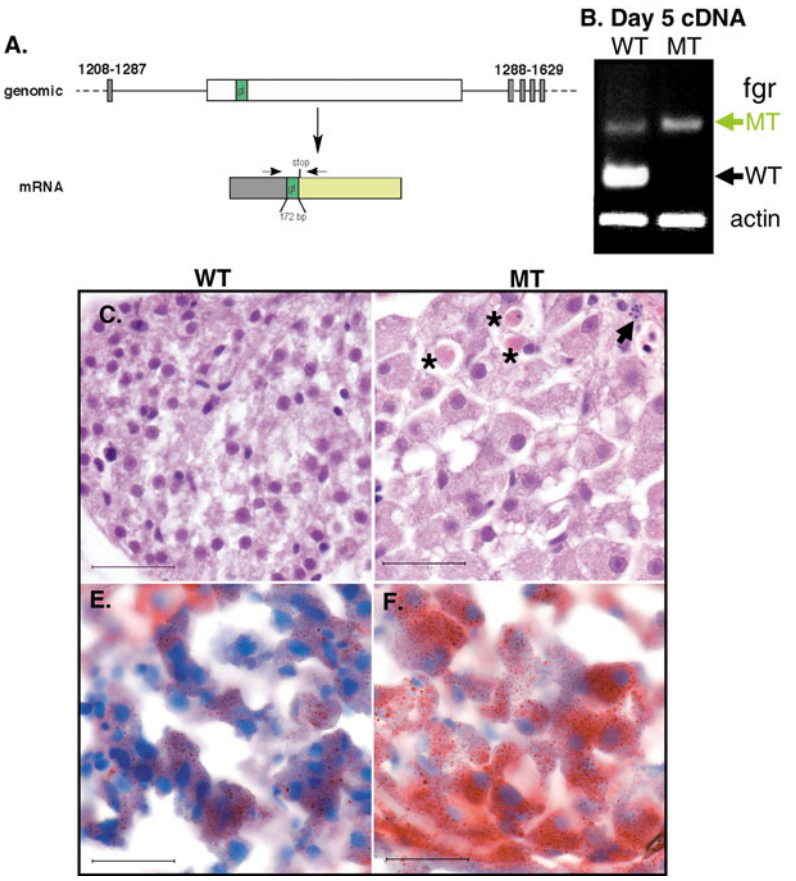

Fig. 8. Mutation of *fgr* causes hepatomegaly and steatosis. (A) The viral insertion (white box) in the intron between exons 11 and 12 of the *fgr* gene in *hi*^{1532B} mutants results in a gene trap cassette of 172 bp (gt, dark green) following bp 1286 of the *fgr*-coding sequence (grey box). The resulting transcript encodes a message that is frame shifted so that a stop codon is created following the gene trap sequence. (B) cDNA prepared from wild-type appearing embryos and their mutant siblings from a hi^{1532B} was amplified with primers that span the trap (arrows on the mRNA diagram in A). As two-thirds of the wild-type appearing embryos from a *hi*^{1532B} clutch are heterozygous for the mutant allele, both transcripts from the trapped allele (green arrow) in addition to transcripts the wild-type allele (black arrow) are amplified in these embryos. The mutant embryos only contain transcripts encoding the trap. Histology from wild-type (C) and mutant (D) day 5 embryos illustrates the large hepatocytes that are filled with vesicles. Several acidophilic bodies (asterisks) representing dead cells as well as those with condensed DNA and nuclear fragmentation (arrow) are evident in mutant livers, but are never observed in wild-type embryos. (E,F) ORO staining of wild-type (E) and mutant (F) livers from day 5 embryos reveals substantial steatosis in *fgr* mutant hepatocytes. Scale bar: 50 μm.

mutant zebrafish embryos, and is consistent with the finding that heterozygous deletion of *nf2* in mice leads to the formation of hepatocellular carcinomas following loss of heterozygosity at the *nf2* locus (McClatchey et al., 1998) and with what is observed in a liver-specific deletion of *nf2* in mice (M., Curto and A. McClatchey, personal communication).

The Nf2 protein merlin is a member of the ERM (ezrin-radixin-moesin) family, which serve as membrane-cytoskeletal linkers. Merlin is thought to be required for contact-mediated inhibition of growth through stabilization of adherens junctions (Lallemand et al., 2003) and also through the inhibition of Pak1 (Kissil et al., 2003). Our preliminary studies indicate that tight junctions are not disrupted in *nf2* mutant livers (K.C.S., unpublished). It is interesting that using RNAi to knock down the levels of a *C. elegans* ERM gene, erm-1, results in the formation of cyst in every tubular epithelial organ in which the gene is normally expressed (Gobel et al., 2004), although junctions are not affected in this model. It will be of interest to examine the structure of the cytoskeleton, junctions and the proliferative index of biliary cells and hepatocytes in *nf2* mutant zebrafish.

Although ARC syndrome and choledochal cysts are relatively rare, steatosis is found in ~25% of the population of the USA, and nearly 1-2% of US citizens have fatty liver disease (Neuschwander-Tetri and Caldwell, 2003), which places it among the most common hepatic pathologies in the developed world (Clark et al., 2002; Neuschwander-Tetri and Caldwell, 2003). Although obesity and excessive alcohol intake are the greatest contributing factors to steatosis and NASH, the clustering of NASH within some families (Struben et al., 2000; Willner et al., 2001) and the numerous mouse models that develop NASH points to a considerable yet varied genetic component to this disease.

We therefore predicted that we might uncover a model of steatosis through a screen for hepatomegaly, but were surprised to find that *fgr* so closely resembles NASH, with the noted exception that there is no inflammation in this mutant. Moreover, as the well-conserved *fgr* gene has no identifiable domains or motifs, it represents a truly novel factor regulating fat accumulation. Multiple molecular pathways, including those controlled by SREBP1-c, PPARγ and insulin are important regulators of hepatic steatosis (Browning and Horton, 2004), and it will be of interest to see whether *fgr* plays a role in any of these pathways.

In summary, by screening for zebrafish mutants with hepatomegaly, novel and physiologically relevant genes underlying embryonic hepatomegaly have been uncovered. We have identified three mutant lines that can serve as valuable models of diseases of lysosomal trafficking, choledochal cyst formation and fatty liver disease. Additionally, several mutants may also provide insight onto the processes that control liver growth and size during development.

This work would not have been possible without the expert assistance of our fish staff, especially S. Farrington and J. Davenport, and the histology core, especially A. Caron. We also thank H. Rennke and C. Ford for their excellence in electron microcopy. The bioinformatics support provided by C. Whittaker and the consultation with the talented pathologists R. Bronson, M. McLaughlin and J. Glickman were invaluable. We are indebted to C. Ukomadu, P. Gissen, A. McClatchy and members of the Hopkins' laboratory for helpful discussions, and to K. Haddix for help with statistics. We are particularly grateful for guidance from J. Lees. K.C.S. was supported by a Ruth L. Kirschstein fellowship from the NICHD (1F32HD042920-01).

References

Amatruda, J. F., Shepard, J. L., Stern, H. M. and Zon, L. I. (2002). Zebrafish as a cancer model system. *Cancer Cell* **1**, 229-231.

Amsterdam, A. and Hopkins, N. (1999). Retrovirus-mediated insertional mutagenesis in zebrafish. *Meth. Cell Biol.* **60**, 87-98.

Amsterdam, A., Burgess, S., Golling, G., Chen, W., Sun, Z., Townsend, K., Farrington, S., Haldi, M. and Hopkins, N. (1999). A large-scale insertional mutagenesis screen in zebrafish. *Genes Dev.* **13**, 2713-2724.

Amsterdam, A., Nissen, R. M., Sun, Z., Swindell, E. C., Farrington, S. and Hopkins, N. (2004). Identification of 315 genes essential for early zebrafish development. *Proc. Natl. Acad. Sci. USA* **101**, 12792-12797.

Behrns, K. E., Shaheen, N. J. and Grimm, I. S. (1998). Type I choledochal cyst in association with familial adenomatous polyposis. *Am. J. Gastroenterol.* **93**, 1377-1379.

Browning, J. D. and Horton, J. D. (2004). Molecular mediators of hepatic steatosis and liver injury. *J. Clin. Invest.* **114**, 147-152.

Clark, J. M., Brancati, F. L. and Diehl, A. M. (2002). Nonalcoholic fatty liver disease. *Gastroenterology* **122**, 1649-1657.

Counce, S. J. (1956). Studies on female-sterility genes in Drosophila melanogaster. I. The effects of the gene deep orange on embryonic development. *Z. Indukt. Abstamm. Vererbungsl.* **87**, 443-461.

Diehl, A. (2001). Alcoholic and non-alcoholic steatohepatitis. In *The Liver: Biology and Pathophysiology* (ed. I. Arias), pp. 738-753. Philadelphia: Lipincott Williams and Wilkins.

Duncan, S. A. (2003). Mechanisms controlling early development of the liver. *Mech. Dev.* **120**, 19-33.

Eastham, K. M., McKiernan, P. J., Milford, D. V., Ramani, P., Wyllie, J., van't Hoff, W., Lynch, S. A. and Morris, A. A. M. (2001). ARC syndrome: an expanding range of phenotypes. *Arch. Dis. Child.* **85**, 415-420.

Farber, S. A., Pack, M., Ho, S. Y., Johnson, I. D., Wagner, D. S., Dosch, R., Mullins, M. C., Hendrickson, H. S., Hendrickson, E. K. and Halpern, M. E. (2001). Genetic analysis of digestive physiology using fluorescent phospholipid reporters. *Science* **292**, 1385-1388.

Field, H. A., Ober, E. A., Roeser, T. and Stainier, D. Y. (2003). Formation of the digestive system in zebrafish. I. Liver morphogenesis. *Dev. Biol.* **253**, 279-290.

Gissen, P., Johnson, C. A., Morgan, N. V., Stapelbroek, J. M., Forshew, T., Cooper, W. N., McKiernan, P. J., Klomp, L. W., Morris, A. A., Wraith, J. E. et al. (2004). Mutations in VPS33B, encoding a regulator of SNARE-dependent membrane fusion, cause arthrogryposis-renal dysfunction-cholestasis (ARC) syndrome. *Nat. Genet.* **36**, 400-404.

Gobel, V., Barrett, P. L., Hall, D. H. and Fleming, J. T. (2004). Lumen morphogenesis in C. elegans requires the membrane-cytoskeleton linker erm-1. *Dev. Cell* **6**, 865-873.

Golling, G., Amsterdam, A., Sun, Z., Antonelli, M., Maldonado, E., Chen, W., Burgess, S., Haldi, M., Artzt, K., Farrington, S. et al. (2002). Insertional mutagenesis in zebrafish rapidly identifies genes essential for early vertebrate development. *Nat. Genet.* **31**, 135-140.

Hemmer, M. J., Courtney, L. A. and Ortego, L. S. (1995). Immunohistochemical detection of P-glycoprotein in teleost tissues using mammalian polyclonal and monoclonal antibodies. *J. Exp. Zool.* **272**, 69-77.

Her, G. M., Chiang, C. C., Chen, W. Y. and Wu, J. L. (2003). In vivo studies of liver-type fatty acid binding protein (L-FABP) gene expression in liver of transgenic zebrafish (Danio rerio). *FEBS Lett.* **538**, 125-133.

Hinton, D. and Pool, C. (1976). Ultrastructure of the liver in channel catfish Ictalurus punctatus (Rafinesque). *J. Fish Biol.* **8**, 209-219.

Hinton, D. and Couch, J. (1998). Architectural pattern, tissue and cellular morphology in livers of fishes: relationship to experimentally-induced neoplastic responses. In *Fish Ecotoxicology* (ed. T. Braunbeck, D. Hinton and B. Streit), pp. 141-164. Basel: Birkhauser Verlag.

Horslen, S. P., Quarrell, O. W. and Tanner, M. S. (1994). Liver histology in the arthrogryposis multiplex congenita, renal dysfunction, and cholestasis (ARC) syndrome: report of three new cases and review. *J. Med. Genet.* **31**, 62-64.

Huizing, M., Didier, A., Walenta, J., Anikster, Y., Gahl, W. A. and Kramer, H. (2001). Molecular cloning and characterization of human VPS18, VPS **11**, VPS16, and VPS33. *Gene* **264**, 241-247.

Iwama, T. (1998). Familial case of choledochocele. *J. Gastroenterol. Hepatol.* **13**, 237.
Iwama, T., Iwata, S., Murakami, S., Ishida, H. and Mishima, Y. (1985). Congenital bile duct dilatation–possibly an hereditary condition. *Jpn J. Surg.* **15**, 501-505.
Iwata, F., Uchida, A., Miyaki, T., Aoki, S., Fujioka, T., Yamada, J., Joh, T. and Itoh, M. (1998). Familial occurrence of congenital bile duct cysts. *J. Gastroenterol. Hepatol.* **13**, 316-319.
Kelly, D. A. and McKiernan, P. J. (1998). Metabolic liver disease in the pediatric patient. *Clin. Liver Dis.* **2**, 1-30.
Kim, B. Y., Kramer, H., Yamamoto, A., Kominami, E., Kohsaka, S. and Akazawa, C. (2001). Molecular characterization of mammalian homologues of class C Vps proteins that interact with syntaxin-7. *J. Biol. Chem.* **276**, 29393-29402.
Kissil, J. L., Wilker, E. W., Johnson, K. C., Eckman, M. S., Yaffe, M. B. and Jacks, T. (2003). Merlin, the product of the Nf2 tumor suppressor gene, is an inhibitor of the p21-activated kinase, Pak1. *Mol. Cell* **12**, 841-849.
Lallemand, D., Curto, M., Saotome, I., Giovannini, M. and McClatchey, A. I. (2003). NF2 deficiency promotes tumorigenesis and metastasis by destabilizing adherens junctions. *Genes Dev.* **17**, 1090-1100.
Lekanne Deprez, R. H., Bianchi, A. B., Groen, N. A., Seizinger, B. R., Hagemeijer, A., van Drunen, E., Bootsma, D., Koper, J. W., Avezaat, C. J., Kley, N. et al. (1994). Frequent NF2 gene transcript mutations in sporadic meningiomas and vestibular schwannomas. *Am. J. Hum. Genet.* **54**, 1022-1029.
Lorent, K., Yeo, S. Y., Oda, T., Chandrasekharappa, S., Chitnis, A., Matthews, R. P. and Pack, M. (2004). Inhibition of Jagged-mediated Notch signaling disrupts zebrafish biliary development and generates multi-organ defects compatible with an Alagille syndrome phenocopy. *Development* **131**, 5753-5766.
Matthews, R. P., Lorent, K., Russo, P. and Pack, M. (2004). The zebrafish onecut gene hnf-6 functions in an evolutionarily conserved genetic pathway that regulates vertebrate biliary development. *Dev. Biol.* **274**, 245-259.
McClatchey, A. I., Saotome, I., Ramesh, V., Gusella, J. F. and Jacks, T. (1997). The Nf2 tumor suppressor gene product is essential for extraembryonic development immediately prior to gastrulation. *Genes Dev.* **11**, 1253-1265.
McClatchey, A. I., Saotome, I., Mercer, K., Crowley, D., Gusella, J. F., Bronson, R. T. and Jacks, T. (1998). Mice heterozygous for a mutation at the Nf2 tumor suppressor locus develop a range of highly metastatic tumors. *Genes Dev.* **12**, 1121-1133.
Moss, J. and Lane, M. D. (1971). The biotin-dependent enzymes. *Adv. Enzymol. Relat. Areas Mol. Biol.* **35**, 321-442.
Nambirajan, L., Taneja, P., Singh, M. K., Mitra, D. K. and Bhatnagar, V. (2000). The liver in choledochal cyst. *Trop. Gastroenterol.* **21**, 135-139.
Narayanan, R., Kramer, H. and Ramaswami, M. (2000). Drosophila endosomal proteins hook and deep orange regulate synapse size but not synaptic vesicle recycling. *J. Neurobiol.* **45**, 105-119.
National Center for Health Statistics (2004). *Health, United States, 2004 With Chartbook on Trends in the Health of Americans.* Hyattsville, MD: US Department of Health and Human Services, Center for Disease Control and Prevention.
Neuschwander-Tetri, B. A. and Caldwell, S. H. (2003). Nonalcoholic steatohepatitis: summary of an AASLD Single Topic Conference. *Hepatology* **37**, 1202-1219.
Newsome, P. N., Hussain, M. A. and Theise, N. D. (2004). Hepatic oval cells: helping redefine a paradigm in stem cell biology. *Curr. Top. Dev. Biol.* **61**, 1-28.
Ober, E. A., Field, H. A. and Stainier, D. Y. (2003). From endoderm formation to liver and pancreas development in zebrafish. *Mech. Dev.* **120**, 5-18.
Pall, H. and Jonas, M. M. (2005). Pediatric hepatobiliary disease. *Curr. Opin. Gastroenterol.* **21**, 344-347.
Peterson, M. R. and Emr, S. D. (2001). The class C Vps complex functions at multiple stages of the vacuolar transport pathway. *Traffic* **2**, 476-486.
Poupon, V., Stewart, A., Gray, S. R., Piper, R. C. and Luzio, J. P. (2003). The role of mVps18p in clustering, fusion, and intracellular localization of late endocytic organelles. *Mol. Biol. Cell* **14**, 4015-4027.
Puckett, L. and Petty, K. (1980). Temperature sensitivity of deep orange: effects on eye pigmentation. *Biochem. Genet.* **18**, 1221-1228.
Raymond, C. K., Howald-Stevenson, I., Vater, C. A. and Stevens, T. H. (1992). Morphological classification of the yeast vacuolar protein sorting mutants: evidence for a prevacuolar compartment in class E vps mutants. *Mol. Biol. Cell* **3**, 1389-1402.
Rocha, E., Monteiro, R. A. and Pereira, C. A. (1994). The liver of the brown trout, Salmo trutta fario: a light and electron microscope study. *J. Anat.* **185**, 241-249.
Rubinstein, A. L. (2003). Zebrafish: from disease modeling to drug discovery. *Curr. Opin. Drug Discov. Dev.* **6**, 218-223.
Ruttledge, M. H., Sarrazin, J., Rangaratnam, S., Phelan, C. M., Twist, E., Merel, P., Delattre, O., Thomas, G., Nordenskjold, M., Collins, V. P. et al. (1994). Evidence for the complete inactivation of the NF2 gene in the majority of sporadic meningiomas. *Nat. Genet.* **6**, 180-184.
Sanson, M., Marineau, C., Desmaze, C., Lutchman, M., Ruttledge, M., Baron, C., Narod, S., Delattre, O., Lenoir, G., Thomas, G. et al. (1993). Germline deletion in a neurofibromatosis type 2 kindred inactivates the NF2 gene and a candidate meningioma locus. *Hum. Mol. Genet.* **2**, 1215-1220.
Sato, T. K., Rehling, P., Peterson, M. R. and Emr, S. D. (2000). Class C Vps protein complex regulates vacuolar SNARE pairing and is required for vesicle docking/fusion. *Mol. Cell* **6**, 661-671.
Sevrioukov, E. A., He, J. P., Moghrabi, N., Sunio, A. and Kramer, H. (1999). A role for the deep orange and carnation eye color genes in lysosomal delivery in Drosophila. *Mol. Cell* **4**, 479-486.
Shestopal, S. A., Makunin, I. V., Belyaeva, E. S., Ashburner, M. and Zhimulev, I. F. (1997). Molecular characterization of the deep orange (dor) gene of Drosophila melanogaster. *Mol. Gen. Genet.* **253**, 642-648.
Sidon, E. W. and Youson, J. H. (1983). Morphological changes in the liver of the sea lamprey, Petromyzon marinus L., during metamorphosis. II. Canalicular degeneration and transformation of the hepatocytes. *J. Morphol.* **178**, 225-246.
Soreide, K., Korner, H., Havnen, J. and Soreide, J. A. (2004). Bile duct cysts in adults. *Br. J. Surg.* **91**, 1538-1548.
Spitsbergen, J. M., Tsai, H. W., Reddy, A., Miller, T., Arbogast, D., Hendricks, J. D. and Bailey, G. S. (2000). Neoplasia in zebrafish (Danio rerio) treated with 7,12-dimethylbenz[a]anthracene by two exposure routes at different developmental stages. *Toxicol. Pathol.* **28**, 705-715.
Sriram, V., Krishnan, K. S. and Mayor, S. (2003). deep-orange and carnation define distinct stages in late endosomal biogenesis in Drosophila melanogaster. *J. Cell Biol.* **161**, 593-607.
Srivastava, A., Woolford, C. A. and Jones, E. W. (2000). Pep3p/Pep5p complex: a putative docking factor at multiple steps of vesicular transport to the vacuole of Saccharomyces cerevisiae. *Genetics* **156**, 105-122.
Struben, V. M., Hespenheide, E. E. and Caldwell, S. H. (2000). Nonalcoholic steatohepatitis and cryptogenic cirrhosis within kindreds. *Am. J. Med.* **108**, 9-13.
Subramanian, S., Woolford, C. A. and Jones, E. W. (2004). The Sec1/Munc18 protein, Vps33p, functions at the endosome and the vacuole of Saccharomyces cerevisiae. *Mol. Biol. Cell* **15**, 2593-2605.
Sun, Z., Amsterdam, A., Pazour, G. J., Cole, D. G., Miller, M. S. and Hopkins, N. (2004). A genetic screen in zebrafish identifies cilia genes as a principal cause of cystic kidney. *Development* **131**, 4085-4093.
Trauner, M. and Boyer, J. L. (2003). Bile salt transporters: molecular characterization, function, and regulation. *Physiol. Rev.* **83**, 633-671.
Trauner, M., Arrese, M., Soroka, C. J., Ananthanarayanan, M., Koeppel, T. A., Schlosser, S. F., Suchy, F. J., Keppler, D. and Boyer, J. L. (1997). The rat canalicular conjugate export pump (Mrp2) is down-regulated in intrahepatic and obstructive cholestasis. *Gastroenterology* **113**, 255-264.
Tuma, P. and Hubbard, A. (2001). The hepatocyte surface: dynamic polarity. In *The liver: biology and pathophysiology* (ed. I. Arias, J. L. Boyer, F. Chisari, N. Fausto, D. Schachter and D. Shafritz), pp. 96-117. Philadelphia: Lippincot Williams and Wilkins.
Ujhazy, P., Kipp, H., Misra, S., Wakabasyasi, Y. and Arias, I. M. (2001). The biology of the bile canaliculus. In *The Liver: Biology and Pathobiology* (ed. I. M. Arias, J. L. Boyer, F. Chisari, N. Fausto, D. Schachter and D. Shafritz), pp. 360-372. Philadelphia: Lippincott Williams and Wilkins.
Wallace, K. N. and Pack, M. (2003). Unique and conserved aspects of gut development in zebrafish. *Dev. Biol.* **255**, 12-29.
Willner, I. R., Waters, B., Patil, S. R., Reuben, A., Morelli, J. and Riely, C. A. (2001). Ninety patients with nonalcoholic steatohepatitis: insulin resistance, familial tendency, and severity of disease. *Am. J. Gastroenterol.* **96**, 2957-2961.